Journal Website: https://www.icjn.net/jswvcm ISSN: 3106-5139 | EISSN: 3106-5147

Journal of Solid Waste Valorization and Chemical Management (JSWVCM)

ICJN Press Volume. 01 | Issue. 02 | Aug. 2026 DOI: 10.66729/jswvcm202606047

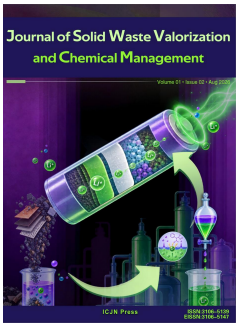

ARTICLE

High-Efficiency Lithium Extraction From Lithium Precipitated Mother Liquor Using the IPE-Z Lithium Extractant Under Weakly Alkaline Conditions

Rongyue Wang[1], Hui Li[1,2], Gaojie Xu[1,*], Pengge Ning[1,3,*]

1 Institute of Process Engineering, Chinese Academy of Science, Beijing 100190, China.
2 School of Chemistry and Biological Engineering, University of Science and Technology Beijing, Beijing 100083, China.
3 University of Chinese Academy of Sciences, Beijing 100049, China.

*Corresponding Author: Gaojie Xu, E-mail: gjxu@ipe.ac.cn; Pengge Ning, E-mail: pgning@ipe.ac.cn

Abstract

As a critical strategic metal, lithium is subject to increasingly stringent resource utilization efficiency requirements. Lithium precipitated mother liquor is the final hurdle in the recovery of lithium resources. Due to its high sodium-to-lithium ratio, strong alkalinity, and complex impurity composition, it poses a significant challenge to the selectivity and stability of traditional extraction systems. In this study, we investigated the influence of different substituents on the enolization capacity of β-diketone extractant molecules based on the electrostatic distribution patterns of extractant molecules. Using this as the primary criterion, we developed a novel extraction system (IPE-Z/tributyl phosphate (TBP)) and examined the effects of various factors, such as pH, extractant concentration, co–extractant ratio and agitation intensity, on extraction yield. Furthermore, the adaptability of this extractant to different feed solutions was verified and its extraction mechanism analysed. The results show that this extractant can achieve over 85% extraction efficiency in a single-stage process and a sodium separation factor ($\beta_{Li/Na}$) of 178.72. Meanwhile, the pH of the extractant raffinate is 7.9, suggesting that lithium can be extracted from lithium–precipitated mother liquor without consuming alkali. In the extractate, the coordination ratio of the extractant molecules, the co-extractant molecules, and the lithium ions is 1:1:1. Infrared spectroscopic analysis of the organic phase before and after extraction confirmed that the extractant's molecular structure remains stable during extraction and back-extraction. Cyclic extraction experiments indicate that this extractant can achieve an extraction efficiency of 98.70% for lithium precipitated mother liquor. The pH of the raffinate is 7.2, enabling the near-neutral extraction of lithium from lithium-precipitated mother liquor, which demonstrates good industrial application prospects.

Keywords

Extraction; Lithium precipitated mother liquor; Lithium recovery; Low-alkali extraction; Resource utilization

Citation: Rongyue Wang, Hui Li, Gaojie Xu, *et al*. High-Efficiency Lithium Extraction From Lithium Precipitated Mother Liquor Using the IPE-Z Lithium Extractant Under Weakly Alkaline Conditions. *Journal of Solid Waste Valorization and Chemical Management*. 2026, 01 (2): 1-15. doi: 10.66729/jswvcm202606047.

Copyright:© 2026 The Author(s). Published by ICJN Press.
This is an open access article under the https://creativecommons.org/licenses/by/4.0/
Received 29 June 2026; Revised 17 July 2026; Accepted 18 August 2026; Available online 28 August 2026.

Graphical Abstract

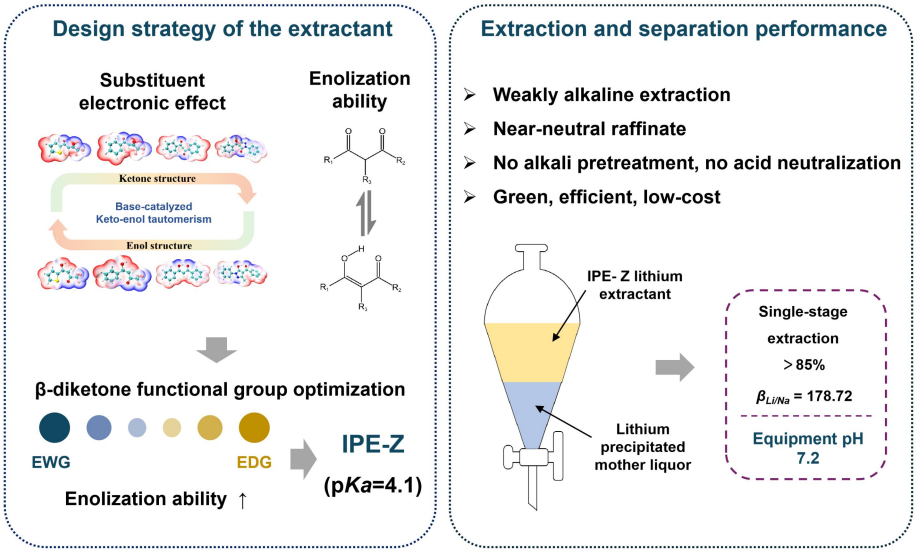

From strong-alkali-driven to weak-alkali-feasible
A breakthrough in alkaline lithium extraction

NOTE: EWG: electron-withdrawing group; EDG: electron-donating group.

Highlights

- A novel lithium extractant, IPE-Z, was designed based on how the electronic properties of various substituents affect the enolization capacity and pKa of β-diketones.
- The IPE-Z extractant achieves a single-stage Li^+ extraction efficiency exceeding 85% under weakly alkaline conditions, demonstrating favorable separation performance.
- This study represents a technological leap from "strong-alkali-driven" to "weak-alkali-compatible" extraction, resolving the bottlenecks of high alkali consumption, excessive salt waste, and elevated treatment costs in conventional processes.

1. Introduction

Lithium, often referred to as "white oil", is a critical metal that is indispensable to the global energy transition[1]. The rapid development of the new energy vehicle industry and the explosive growth of the energy storage market have made the strategic importance of lithium resources increasingly prominent. According to statistics from the Lithium Industry Branch of the China Nonferrous Metals Industry Association, China's lithium carbonate production capacity reached 1.78 million metric tons by 2025, with output reaching 97.60 metric tons — a year-on-year increase of 39.30%[2]. Against the backdrop of rapid capacity expansion, the issue of resource utilization efficiency in the lithium carbonate production process has become increasingly important.

The carbonate precipitation method is currently the mainstream process for extracting lithium from salt lake brine and lithium ore. However, due to the limited solubility of lithium carbonate, the recovery rate for lithium precipitation in a single pass is only around 80%, resulting in approximately 20% of the lithium being lost in the mother liquor from the precipitation process. These mother liquors constitute a complex, highly saline and alkaline brine system, containing lithium-ion concentrations ranging from 0.50 g/L to 3 g/L and sodium ion concentrations of up to 45 g/L–60 g/L. The direct discharge of these mother liquors results in the significant waste of lithium resources and generates large volumes of salt-containing waste liquid, creating environmental pollution pressures[3-7]. Of the many lithium extraction methods, solvent extraction is considered a separation technology with significant industrial potential thanks to its many advantages, such as high processing capacity, excellent selectivity, straightforward operation and ease of scaling up. Lithium extractants are classified into two categories depending on the properties of the target feed solution: acidic (primarily tributyl phosphate (TBP) and $FeCl_3$) and basic (primarily β-diketones)[8]. Regarding alkaline feed systems, such as lithium precipitation mother liquors, researchers have conducted extensive studies on various alkaline extractants, including β-diketones, organophosphorus compounds, crown ethers, ionic liquids, and eutectic solvents[9,10].

Traditional extraction processes for efficient lithium recovery from lithium precipitation mother liquors often require operation under highly alkaline conditions, consuming large amounts of alkaline reagents such as sodium carbonate. This generates significant amounts of waste salt and saline wastewater, substantially increasing companies' environmental treatment costs and solid waste disposal pressures[11-13]. Therefore, developing new extractants that can efficiently extract lithium under low-alkalinity conditions, thereby reducing alkali consumption and salt waste emissions at source, is a key breakthrough for improving the

comprehensive recovery rate of lithium resources. It is also an urgent requirement for transitioning lithium carbonate production towards a green, low-carbon model. This study addresses this objective by focusing on lithium-precipitation mother liquors to develop a novel, low-alkalinity extraction system that aims to synergistically integrate efficient lithium recovery with clean production.

Extractants based on β-diketones have long been the focus of research for the extraction of Li^+ from alkaline lithium-containing solutions, such as salt lake brine, lithium-precipitation mother liquors and waste battery recycling solutions, due to their superior ability to recognize and separate lithium ions compared to other alkali metal ions, particularly Na^+[14,15]. Their extraction mechanism is based on the fact that β-diketones undergo isomerization from the ketone form to the enol form under alkaline conditions. After the hydroxyl group is hydrolyzed, the Li^+ chelates with the two oxygen atoms of the enol form, thereby forming a stable six-membered ring structure[16]. This process usually involves organophosphorus compounds (e.g., trioctylphosphine oxide (TOPO), trialkylphosphine oxide (TRPO), and TBP acting as synergistic extractants. The P=O group of the organophosphorus compound interacts electrostatically with Li^+, thereby enhancing the stability and hydrophobicity of the complex and significantly improving extraction efficiency[16,17].

Early studies have shown that fluorinated β-diketones, such as 4,4,4-Trifluoro-1-phenyl-1,3-butanedione (HBTA) and 2-Thenoyltrifluoroacetone (HTTA), can achieve highly selective extraction of lithium under highly basic conditions (pH greater than 11) due to the strong electron-withdrawing effect of their trifluoromethyl groups. However, this extraction method requires large amounts of base and results in significant dissolution losses of the extractant[15,17]. Non-fluorinated β-diketones (such as 1-phenyl-3-heptyl-1,3-propanedione (PHPD)) also require extremely alkaline conditions (pH > 13) to achieve satisfactory extraction yields[18]. In recent years, researchers have attempted to address the economic and environmental issues associated with high alkalinity by optimizing molecular structures to lower the required extraction pH. For example, combining a pyrazolone moiety with a β-diketone structure and introducing novel extractants containing nitro groups and long alkyl groups has successfully lowered the semi-extraction pH to 8.5–9.5, significantly reducing alkali consumption and extractant loss[19,20].

This study aimed to address the issues of high equilibrium pH and high alkali consumption in traditional extraction systems, as well as the large quantities of mixed-salt solid waste generated when lithium is precipitated from mother liquor. To accomplish this, a novel lithium extractant called IPE-Z was developed and its extraction and separation capabilities were verified under weakly alkaline conditions. This study investigated the optimal process conditions for extraction, washing and reverse extraction based on actual industrial production processes. The extraction efficiency was systematically evaluated and the process route was validated using actual feedstock solutions. The results have overcome the reliance on strong alkalis in traditional systems by shifting the operational pH range for alkaline extraction towards neutral conditions. The results of these studies provide valuable technical information and theoretical support for developing highly efficient lithium extraction technologies and for the efficient recycling of lithium-precipitated mother liquors under weakly alkaline conditions.

2. Methods

2.1 Calculation

This study employed density functional theory (DFT) to perform computational analyses of the molecular structures of four typical β-diketones. All DFT calculations were performed using Gaussian 16 at the B3LYP/6-311G** level of theory[21]. The SMD implicit solvation model with n-dodecane (ε = 2.0060) as the solvent was employed to simulate the organic phase environment. Frequency calculations were conducted at the same level of theory to confirm that all optimized structures correspond to true energy minima on the potential energy surface (no imaginary frequencies). All quantum chemical calculations were performed using Gaussian 16[21]. The Multiwfn software was then used to analyze the surface charge distribution characteristics of molecules with different conformations, revealing differences in the alkalinity requirements for the extraction process among various extractant molecules[22-25].

2.2 Experimental

2.2.1 Reagents and Instruments

The chemicals used to prepare the simulated feed solutions in this study included H_2SO_4 (98%), Na_2CO_3 (99%), Na_2SO_4 (99%), Li_2SO_4 (99%), K_2SO_4 (99%), and TBP (98%), among others. These were obtained from Aladdin Industry Corporation and Sinopharm Chemical Reagent Co., Ltd., respectively. The composition of the simulated feed solution is shown in **Table 1**. The lithium precipitated mother liquor used in the extractant circulation validation experiments was provided by a domestic company, and its specific composition is shown in **Table 2**. The extractant used in this study was a newly designed and developed lithium extractant designated IPE-Z. Tributyl phosphate (TBP, AR) procured from Aladdin Industry Corporation (Shanghai, China) and Sinopharm Chemical Reagent Co., Ltd. (Beijing, China), was used as the co-extractant. The diluent was sulfonated kerosene, procured from Sannuo New Materials Technology (Luoyang) Co., Ltd. (Luoyang, China).

Table 1. The composition of the simulated feed solution

Elements	Li	Na	K	CO_3^{2-}
Concentration (g/L)	2.55−2.84	59.68−75.37	8.55−12.23	7.719−22

Table 2. The composition of lithium-precipitated mother liquor

Elements	Li	Na	K	CO_3^{2-}	pH
Concentration (g/L)	2.62	59.35	11.74	14.59	11.08

For the extraction condition experiments in this study, a Model 1335-2E double-deck shaking incubator was used to

maintain a temperature of 25 °C. A custom-built continuous extraction apparatus (Jiangsu Zhengfen Technology Co., Ltd., Nanjing, China) was used for the cyclic extraction experiments. The concentrations of metal ions (Li^+, Na^+, and K^+) in the aqueous phase were determined using an ICP-OES spectrometer (Model 5,800, Agilent Technologies Inc., Santa Clara, California, USA). The concentrations of CO_3^{2-} and other ions in the solutions were measured by titration. The pH values of the solutions were measured using a pH meter (INESA Scientific Instrument Co., Ltd., Shanghai, China). The chemical oxygen demand (COD) of the solutions was determined with a rapid COD digestion and analysis system (Beijing Lianhua Yongxing Technology Development Co., Ltd., Beijing, China). Fourier-transform infrared (FTIR) spectra were recorded using a Bruker INVENIO S infrared spectrometer (Bruker Optik GmbH, Ettlingen, Germany).

2.2.2 Extraction Experiment

The extraction agents were prepared by dissolving IPE-Z and TBP in sulfonated kerosene at different concentrations. The extraction agent (the organic phase) was mixed with the lithium-containing solution (the aqueous phase) at the desired volume ratio. The mixture was then agitated in a shaker at 200 rpm and 25 °C for 5 minutes. The mixture was then left to stand for 10 minutes, after which the aqueous phase was removed for analysis. During the extraction process, Na_2CO_3 and NaOH were used to adjust the pH of the lithium-containing solution. The formulas for calculating the extraction efficiency, distribution ratio, and separation factor during the extraction process are as follows:

$$E_i = \frac{c_{i,o} V_o}{c_{i,A} V_A} \quad (1)$$

$$D_i = \frac{c_{i,o}}{c_{i,A}} \quad (2)$$

$$\beta_{i/j} = \frac{D_i}{D_j} \quad (3)$$

Where, $C_{i,O}$ and $C_{i,A}$ represent the concentrations of component i in the organic and aqueous phases, respectively. V_O and V_A represent the volumes of the organic and aqueous phases, respectively. E_i is the extraction rate of component i, D_i is its distribution ratio, and $\beta_{i/j}$ is the separation factor between components i and j.

Sulfuric acid was used to prepare both the washing solution and the counter-extraction agent. Sulfuric acid solutions of varying concentrations were prepared for the washing and counter-extraction processes in order to determine the optimal conditions. The mixing ratio for both processes was 10:1, with all other conditions remaining consistent with those used for extraction.

3. Result and Discussion

3.1 β-Diketone Structures and Electrostatic Potential

The ketone-enol tautomerism characteristic of β-diketones significantly influences their acidity and ability to coordinate metals. Three typical β-diketone extractants — HTTA, HBTA, dibenzoylmethane (HDBM, abbreviated as DBM) and 4-Benzoyl-3-methyl-1-phenylpyrazol-5-one (HPMBP) — were selected for analysis to investigate their enolization processes. First, the energy differences between the ketone and enol forms were compared, as well as the changes in surface electrostatic potential distribution, for the four compounds. As demonstrated in **Figure. 1**, when dissolved in a solvent, both HTTA and HBTA are found to be present primarily in their ketone form. However, the enol transformation, which involves a shift in configuration, requires the input of additional energy to be initiated. On the other hand, HDBM and HPMBP exhibit a higher propensity for undergoing this enol transformation. These differences are primarily attributed to the varying electronic effects of the different substituents. The two phenyl substituents on HDBM effectively stabilize the enol configuration through conjugation effects[26]. The pyrazoline ring system in HPMBP provides a more extensive π-conjugated delocalization pathway, thereby maximizing the stabilization of the enol form. In contrast, both HTTA and HBTA contain the strongly electron-withdrawing trifluoromethyl (-CF_3) substituent, which should theoretically promote an increase in enol content[27].

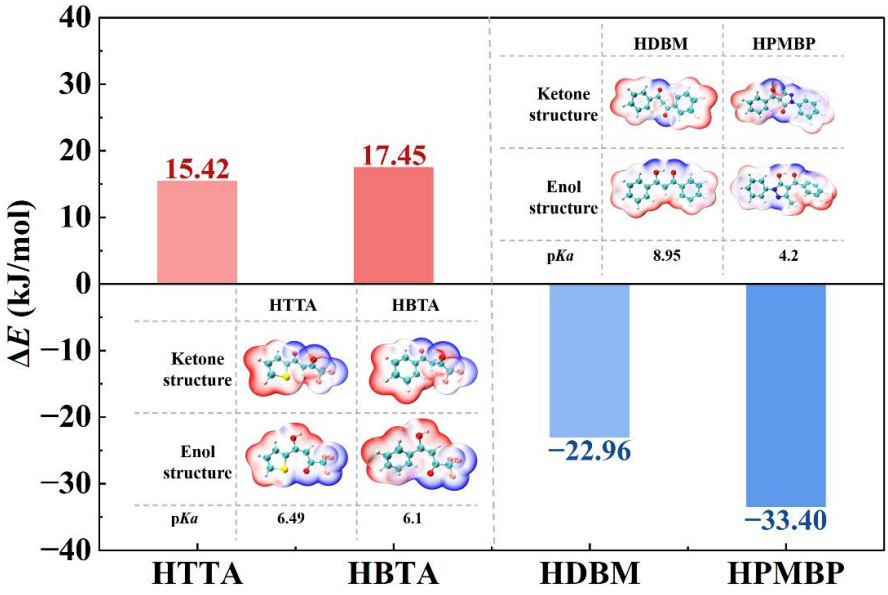

Figure. 1 Comparison of the ketone-to-enol transition capabilities and the electrostatic potential (ESP) analysis of HTTA, HBTA, HDBM, and HPMBP. **NOTE:** HTTA: 2-Thenoyltrifluoroacetone; HBTA: 4,4,4-Trifluoro-1-phenyl-1,3-butanedione; HDBM: Dibenzoylmethane; HPMBP: 4-Benzoyl-3-methyl-1-phenylpyrazol-5-one. Copyright: Created by the authors using Origin 2026 and VMD[25] software.

The electrostatic potential (ESP) analysis revealed the characteristics of charge redistribution on the molecular surface during interconversion: during the transition from ketone to enol form, the ESP distributions of HTTA and HBTA shifted towards the positively charged blue region. This indicates a reduction in negatively charged regions on the molecular surface and a decrease in overall electron density. This is consistent with calculation results showing a positive ΔE for both compounds (the enol form has a higher energy), which reflects the fact that in a polar solvent environment, the transition from the ketone form to the enol form is accompanied by a redistribution of electron density and a weakening of the solvent-stabilizing effect. Conversely, the blue regions of the ESP for HDBM and HPMBP decreased slightly during enolization, suggesting an increase in negative charge on the molecular surface or a more delocalized electron density distribution. This is consistent with computational results showing a negative ΔE for both compounds (the enol form is more stable), confirming that the negative charge in their enol structures is dispersed and stabilized effectively through an extended π-conjugated system. This is particularly true for HPMBP, whose pyrazolone ring system provides a more effective charge delocalization pathway, resulting in the enol form being optimally stable in terms of both energy and electronic structure[28].

The electrostatic potential minima in the regions of the oxygen atoms of four β-diketone enol anions (L^-) were compared, and their ligand activity evaluated. The results are shown in the **Figure. 2**: lithium-ion coordination typically occurs near the enolized oxygen carbonyl group. The greater the electronegativity in this region, the stronger the ability to coordinate lithium ions[29]. HDBM and HPMBP have a higher affinity for lithium ions than HTTA and HBTA. HTTA and HBTA both contain the strongly electron-withdrawing trifluoromethyl ($-CF_3$) substituent. Through inductive effects, this pulls electron density away from the region of the oxygen atom, resulting in reduced localized negative charge density near the oxygen atom. Meanwhile, the thiophene ring in HTTA has some electron-donating properties, giving it a slightly more negative electrostatic potential than HBTA. The HDBM molecule exhibits high symmetry, with equivalent chemical environments around the two oxygen atoms. The negative charge of the enolate anion is uniformly distributed between the two oxygen atoms, with only one point of maximum charge, which makes HDBM more negative. However, HPMBP is more prone to enolization reactions.

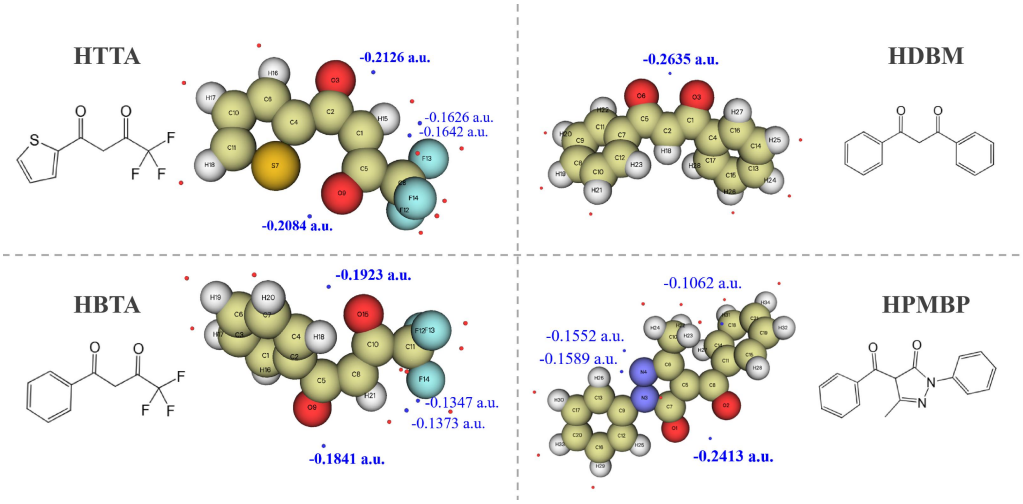

Figure. 2 Comparison of the electronegativity of the coordinating oxygen atoms in the enolate anions of HTTA, HBTA, HDBM and HPMBP. Copyright: Created by the authors using Multiwfn and Microsoft PowerPoint.

According to the literature[30-32], the p*Ka* values of the four compounds shown in **Figure. 1** reveal how the electronic effects of different substituents influence the acidity of β-diketones. The fluorine substituent ($-CF_3$) significantly reduces the p*Ka* value due to its strong electron-withdrawing effect (HTTA , 6.49). Aromatic ring substituents stabilise the enolate anion via conjugation effects (HDBM, 8.95), while the pyrazoline ring system provides a more effective route for charge delocalisation (HPMBP, 4.2), resulting in the lowest p*Ka* value. This sequence of p*Ka* values closely correlates with the order of extraction performance among the four model compounds.

These findings have enabled this study to identify the core concept of molecular design. By introducing substituents with the appropriate electron-donating effects, the energy barrier for enolisation is lowered, making the enol form more stable. At the same time, the electron density in the region of the coordinating oxygen atom increases, enhancing the extractant's ability to coordinate with Li^+ under lower pH conditions.

Based on this approach, our research team modified the extractant molecules by controlling different substituents to enhance their enolization capacity and coordination ability. We designed and developed an extractant named IPE-Z (β-diketones, with a p*Ka* of 4.1) and conducted a systematic study of its lithium extraction performance under weakly basic conditions.

3.2 Extraction Efficiency Under Different Alkaline Conditions

The feasibility of using the IPE-Z extractant for lithium extraction under weakly alkaline conditions was analyzed. The extractant concentration was set to 0.4 mol/L, and the lithium-containing solution contained 2.84 g/L of Li^+, 75.37 g/L of Na^+, 12.23 g/L of K^+, and 22 g/L of CO_3^{2-}. A 6 mol/L NaOH solution was used to adjust the pH of the lithium-containing solution and investigate the extractive separation efficiency of the extractant at different alkali concentrations. The amount of alkali added was based on the molar ratio of OH^- in the adjustment solution to Li^+ in the feed solution.

As shown in the **Figure. 3**, the single-stage extraction efficiency

for lithium always exceeded 85%. During the extraction process, carbonate ions were consumed, resulting in a lower equilibrium pH at the end of the extraction process than at the beginning. Without the addition of a buffer solution, the equilibrium pH at the extraction stage was 7.9, and the extractant was still capable of efficiently separating lithium. When the alkali: lithium ratio reached 1.2, there was little difference in pH between the pre-extraction and post-extraction stages. The alkalinity required for the extraction reaction is significantly lower than that required for traditional β-diketone extractants (see **Table 3** and **Table 4**). Several currently mainstream extractants, such as Lix54 and HBTA, require highly alkaline conditions (equilibrium pH ≥ 10) to achieve high lithium extraction efficiency[33-37]. Alternatively, under conditions of low lithium concentration (lithium concentration was approximately 0.10 g/L–0.50 g/L), they require an increased extractant concentration to achieve high extraction rates. However, their performance is suboptimal under conditions of higher lithium concentration and lower pH. In contrast, the extractant developed in this study continues to demonstrate excellent extraction performance under these conditions, suggesting its potential for lithium extraction under weakly alkaline conditions.

Table 3. Li/Na separation factors under different alkaline conditions

NaOH Addition Amount(n_{Na}:n_{Li})	0	0.20	0.40	0.60	0.80	1	1.20	1.40	1.60
$\beta_{Li/Na}$	178.72	88.59	∞	∞	∞	∞	∞	∞	∞
$\beta_{Li/K}$	2359.64	57.12	∞	162.64	269.19	∞	2310.82	∞	146.46

Table 4. Extraction performance of various extractants on lithium-containing solutions, such as lithium-precipitated mother liquors, as reported in the literature

Extractant	Lithium Solution	E_{Li}	Initial pH	Equilibrium pH	$\beta_{Li/Na}$
IPE-Z/TBP (This study)	Li: 2.84 g/L Na: 75.37 g/L	85.30%	12.04	7.90	178.72
Lix54 and Cyanex923[33]	Li: 2.20 g/L Na: 35 g/L	67.37%	/	12.06	＞60
PHPD and Cyanex923[18]	Li: 1.39 g/L Na: 68.97 g/L	97.83%	13.06	/	475.60
DBM and TBP[34]	Li: 2.10 g/L Na: 70.99 g/L	99.96%	/	＞10	5320
HBTA and TBP[35]	Li: 0.48 g/L Na:101.30 g/L K:5.56 g/L	70.94%	8.96	7.93	≈ 180
TBP-HDES[36]	Li: 1.48 g/L Na: 55.27 g/L	56.20%	/	/	20.50
HBTA and TOPO[15]	Li: 0.138 g/L	＞90%	13	＞11	/
HBTA and TRPO[37]	Li: 1.80 g/L Na: 65 g/L K: 1.51 g/L	90.90%	/	11.02	335

NOTE: TOPO: rioctylphosphine oxide; TRPO: trialkylphosphine oxide; TBP: tributyl phosphate; PHPD: 1-phenyl-3-heptyl-1,3-propanedione; DBM: dibenzoylmethanate.

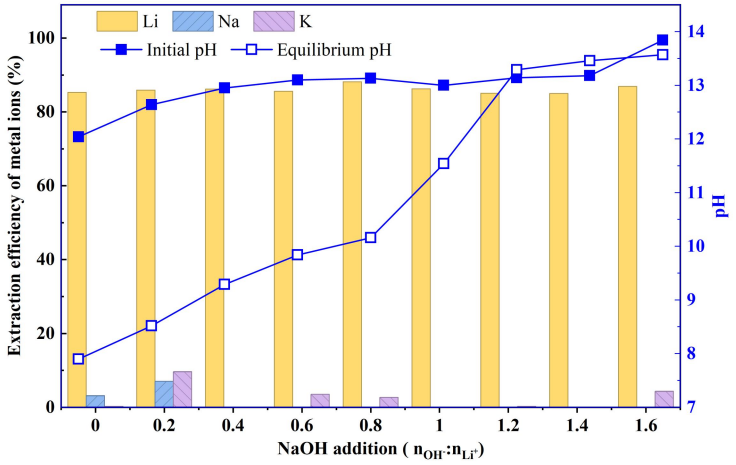

Figure. 3 Li extraction efficiency under different alkaline conditions. Copyright: Created by the authors using Origin 2026 software.

3.3 Extraction Mechanism

3.3.1 Slope Analysis for Extraction

The ratio of extractant molecules to co-extractant molecules participating in the reaction during the extraction process can be determined using the slope method[38]. The extraction reaction equation was:

$$Li^+ + x\ IPE\text{-}Z + y\ TBP = Li[IPE\text{-}Z]x\ [TBP]y + z\ H^+ \quad (4)$$

Derivation based on the thermodynamic equilibrium equations:

$$Log\ D_{Li} = x\ Log\ [IPE\text{-}Z] + y\ Log\ [TBP] - z\ Log\ [H^+] + C \quad (5)$$

The distribution coefficient D_{Li} of Li between the aqueous and organic phases was analyzed by adjusting the pH of the lithium-containing solution with NaOH and varying the concentrations of IPE-Z and TBP in the extractant, respectively. A linear fit was performed for Log D_{Li} against pH, Log [IPE-Z], and Log [TBP] (**Figure 4**). The fitted values of the slope correspond to x, y, and z in equation (5), that is, x = 1.02179, y = 0.94299, and z = 1.01233. This result indicated that one Li^+ ion coordinated with one IPE-Z extractant molecule and one TBP co-extractant molecule to form a complex. Therefore, equation (4) could be written as follows:

$$Li^+ + IPE\text{-}Z + TBP = Li[IPE\text{-}Z][TBP] + H^+ \quad (6)$$

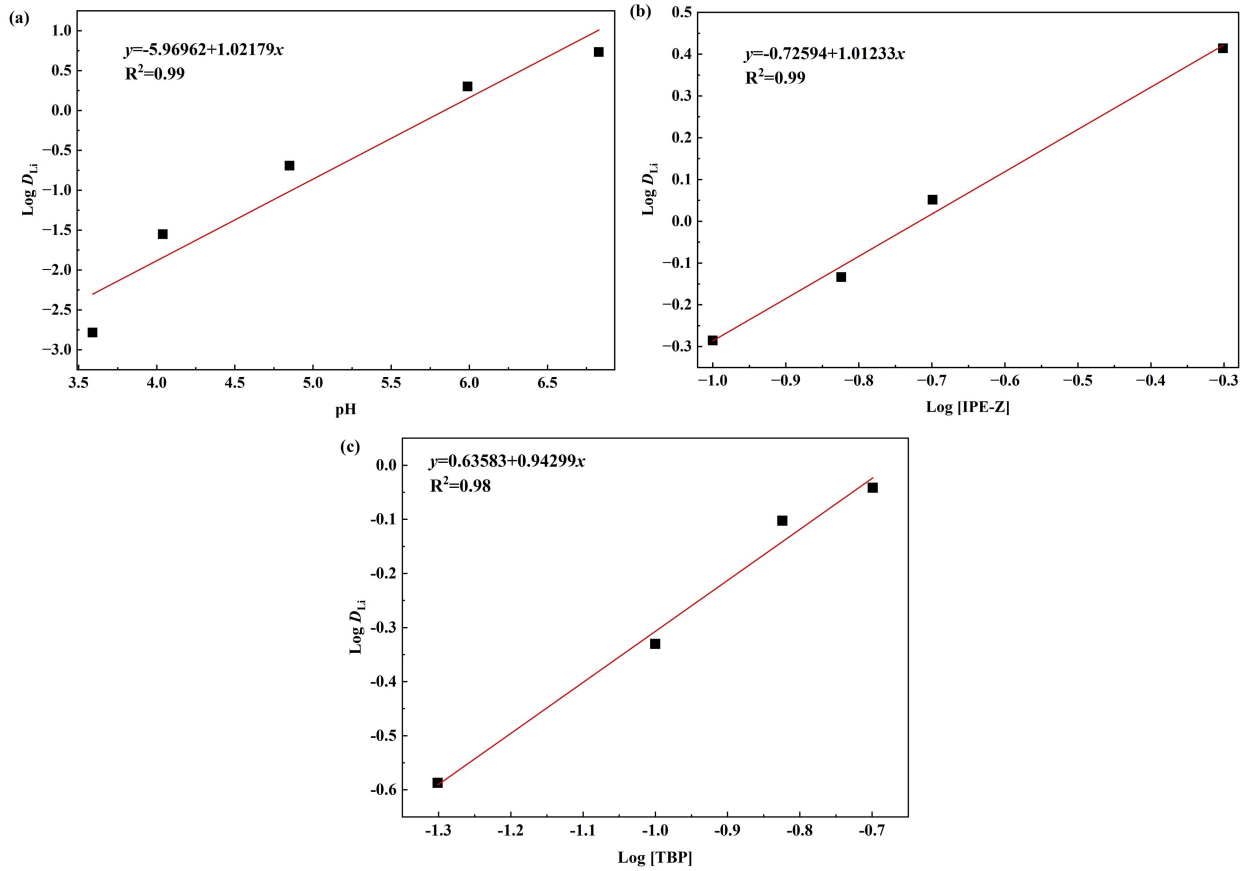

Figure. 4 Linear fitting of Log D_{Li} against. (a) pH (Log [H+]); (b) Log [IPE-Z]; (c) Log [TBP] for the determination of the stoichiometric coefficients in the Li^+ extraction reaction. **NOTE:** TBP: tributyl phosphate. Copyright: Created by the authors using Origin 2026 software.

3.3.2 Driving Forces of Extraction Reactions

The extraction process involved varying the concentrations of the extractants in solutions with low Li concentrations. The aqueous phases used for the extraction process were LiOH and Li_2CO_3 solutions. The extraction capacities of OH^- and CO_3^{2-} at different concentrations were compared with their respective consumption rates in order to investigate the driving forces of the extraction process, determine the required levels of CO_3^{2-} and OH^-, and quantify the theoretical alkali consumption during extraction. For carbonate-type solutions, the following hydrolysis reaction occurs:

$$CO_3^{2-} + H_2O = HCO_3^- + OH^- \quad (7)$$

$$HCO_3^- + H_2O = H_2CO_3 + OH^- \quad (8)$$

The base requirement is determined by the sum of the amount of carbonate ions converted to bicarbonate ions in the Li_2CO_3 solution and the original amount of OH^- in the solution. The results are shown in the **Figure. 5**. The ratio of extractant concentration to the amount of OH^- consumed during the extraction process is approximately 1:1. When the extractant concentration is low and the TBP concentration is also low, lithium cannot be completely extracted, and the ratio of Li^+ loaded in the organic phase to the consumed OH^- is less than 1. This indicates that the extraction process consumes additional OH^-. At different IPE-Z concentrations, the ratio of Li^+ loaded in the organic phase to the consumed OH^- remains stable at around 1.

At low concentrations, the Li^+ concentration in the solution exceeds the extractant concentration. After TBP, IPE-Z, and Li^+ form a 1:1:1 coordination complex at low concentrations, additional OH^- is still consumed.

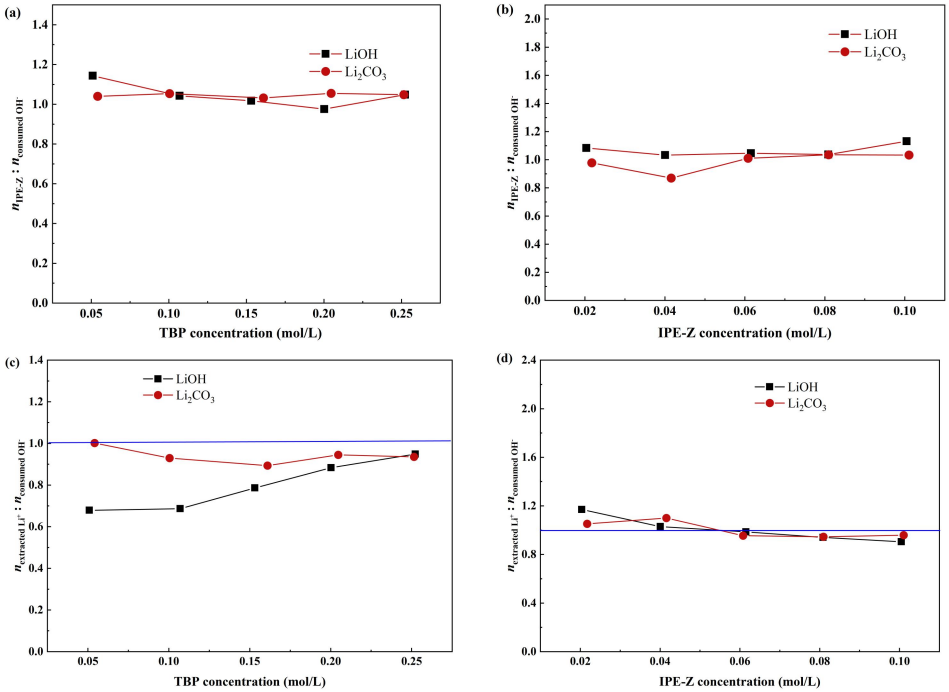

Figure. 5 OH^- and CO_3^{2-} requirements for the extraction process. (a) Extractant concentration versus OH^- consumption at various TBP concentrations; (b) Extractant concentration versus OH^- consumption at various IPE-Z concentrations; (c) Amount of Li^+ extracted versus OH^- consumption at various TBP concentrations; (d) Amount of Li^+ extracted versus OH^- consumption at various IPE-Z concentrations. Copyright: Created by the authors using Origin 2026 software.

3.3.3 The Effect of Extractant Concentration

Extractants with concentrations of 0.05 mol/L, 0.10 mol/L, 0.15 mol/L, 0.20 mol/L, and 0.50 mol/L were prepared. The concentration ratio of the primary extractant to the co-extractant was 1:1. The extraction ratio was set to 1 and the extraction process was carried out under the conditions described in Section 2.2.

Figure. 6 shows the results of lithium extraction and separation. The lithium extraction rate increases as the extractant concentration increases. As discussed earlier, based on the results, the extractant molecules coordinate with lithium ions in a 1:1 ratio. The dashed line in the figure shows the theoretical extraction rate when the extractant is fully loaded with lithium, calculated based on the extractant concentration. When the solvent concentration is lower than the lithium concentration in the aqueous phase, the actual extraction efficiency of lithium differs only slightly from the theoretical efficiency. When the solvent concentration exceeds the lithium concentration in the aqueous phase, the single-stage extraction efficiency is 72.24%. However, at higher extractant concentrations, intermediate products precipitate during the extraction process. This phenomenon can be mitigated by adding a co-extractant.

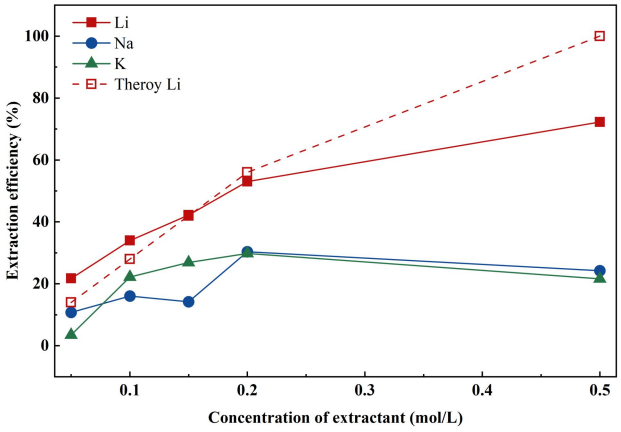

Figure. 6 Effect of different extraction agent concentrations on the extraction and separation of lithium from simulated feed solutions. Copyright: Created by the authors using Origin 2026 software.

3.3.4 The Effects of Co-extraction Ratios

The effects of different TBP concentrations on extraction efficiency were investigated under under-stoichiometric (0.20 mol/L) and stoichiometric (0.50 mol/L) conditions. As shown in the **Figure. 7**, the solid-phase precipitation still occurred during the extraction process when the co-extractant ratio was ≤ 2; however, this phenomenon disappeared when the ratio exceeded 3. As the co-solvent ratio increased, the extraction rate of Li remained relatively unchanged. Conversely, when the extractant was in a sub-stoichiometric state, the extraction rates of Na^+ and

K^+ were lower under all ratio conditions. However, when the ratio increased to 4 or higher under conditions of excess extractant, the extraction rates of Na^+ and K^+ decreased. Furthermore, based on the COD results of the extractant raffinate, COD decreased as the co-extractant ratio increased, indicating less dissolution loss during the extraction process. Overall, the extractant system was more stable when the co-extractant ratio was ≥ 4.

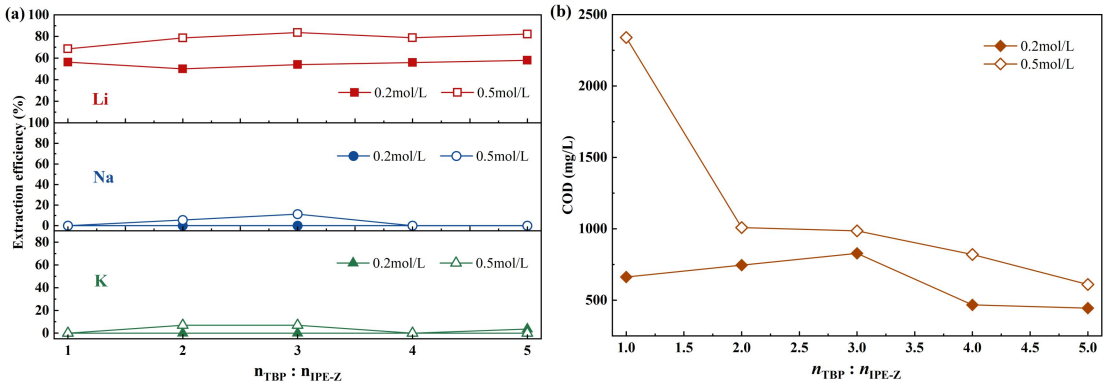

Figure. 7 Extraction performance and extractant dissolution loss as a function of IPE-Z: TBP molar ratio. (a) Extraction efficiencies of Li^+, Na^+, and K^+; (b) COD values of the raffinate. **NOTE:** COD: chemical oxygen demand. Copyright: Created by the authors using Origin 2026 software.

3.3.5 Analysis of Extracts

To investigate changes to the extractant's structure during the extraction process, Fourier transform infrared spectroscopy (FTIR) was used to compare the organic phases before and after extraction. The results are shown in the **Figure. 8**. Both sets of spectra exhibited strong C–H stretching vibrations from methyl and methylene groups at 2,958 cm^{-1}, 2,923 cm^{-1}, and 2,853 cm^{-1}. The positions of the bending vibration peaks at 1,459 cm^{-1} and 1,377 cm^{-1} were consistent, indicating that the ligand's long-chain alkane backbone remained intact during the extraction process and that no degradation or cleavage occurred.

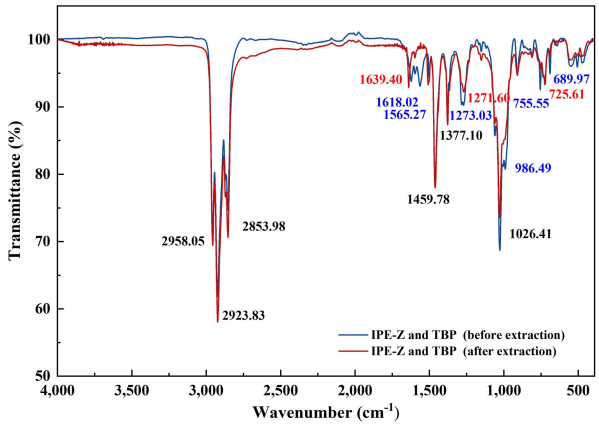

Figure. 8 FTIR analysis of the extraction solvent before and after extraction. Copyright: Created by the authors using Origin 2026 software.

The absorption bands at 1,618 cm^{-1} and 1,565 cm^{-1} in the pre-extraction sample are attributed to coupled vibrations of conjugated enolic C=C and C=O bonds in the free β-diketone ligand. In the post-extraction sample, these two peaks disappear, and a new, broad absorption band appears at 1639 cm^{-1}. This significant blue shift ($\Delta\nu \approx 21$ cm^{-1}–74 cm^{-1}) is due to the β-diketone ligand coordinating with the Li^+ ion following deprotonation to form a stable, six-membered, chelating ring structure. This results in the rearrangement of the conjugated system and redistribution of electron density, causing the carbonyl vibration frequency to shift towards higher wavenumbers.

The characteristic double peak of the out-of-plane bending vibration of the C–H bond in a monosubstituted benzene ring was observed at 755 cm^{-1} and 690 cm^{-1} in the sample prior to extraction; after extraction, this merged and shifted to 725 cm^{-1}. The formation of the chelate ring stiffens the molecular spatial configuration. At the same time, the tight ion pair formed upon coordination with the lithium ion affects the crystal field effects around the benzene ring. This causes the originally split out-of-plane bending vibration to become degenerate or shift, leading to coupling and overlap with the in-plane wagging vibration of the long-chain methylene group, which is typically located near 720 cm^{-1}.

In addition, both samples exhibited absorption peaks at 1,271 cm^{-1} (P=O stretching vibration) and 1,026 cm^{-1} (P–O–C stretching vibration). However, the slight shift in peak positions following extraction suggests that TBP molecules are involved in forming the lithium ion's solvation shell or the outer layer of the chelate complex via coordination or hydrogen bonding. During extraction, the β-diketone ligand transitions from a free state to a Li^+-chelated state, with the extractant molecule's main structural integrity remaining intact.

3.4 Extraction Process Parameters

3.4.1 Extraction Conditions

During the extraction process, shaking speed and duration are critical parameters affecting the mixing, mass transfer and extraction equilibrium of the aqueous and organic phases. With the phase ratio (O/A = 1), pH value, temperature and other

operating conditions kept constant, the single-stage extraction efficiency was investigated under various shaking speeds and durations. The corresponding results are presented in the **Figure. 9**.

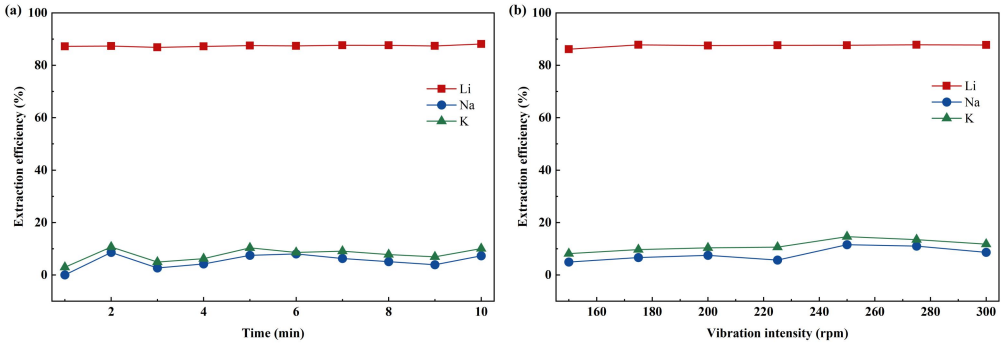

Figure. 9 Effect of agitation conditions on lithium extraction efficiency. (a) Agitation time; (b) Agitation intensity (rotation speed). Copyright: Created by the authors using Origin 2026 software.

Lithium exhibits a fast extraction kinetic rate, and extraction equilibrium can be reached at low shaking speeds within a short time. Changes in the above two factors barely affect the extraction efficiency of lithium. By contrast, the extraction rates of impurity ions sodium and potassium increase slightly with the rise of shaking speed, with an increment of less than 5% for both ions. When the shaking duration is prolonged, the extraction rates of sodium and potassium fluctuate mildly within a range below 8%. Despite the slight increase in the extraction rates of impurity ions, such increments are negligible. These impurities can be effectively removed via washing in the subsequent processes. Accordingly, the extractant possesses excellent selectivity toward lithium and favorable extraction kinetics. In practical application, efficient lithium extraction can be realized at low stirring intensity and short extraction time.

3.4.2 Compatibility of the Extractant

The saturation capacity of the extractant was verified through a three-stage cross-flow extraction experiment. The results are shown in **Table 5**. The extraction rate of Li in the first stage was 84.40%; it decreased to 39.68% in the second stage and further dropped to 2.56% in the third stage, at which point almost no extraction occurred. The saturation capacity of the extractant was approximately 3.06 g/L.

The effect of phase ratio on extraction efficiency was investigated, and the results are presented in the **Figure. 10(a)**. With the gradual increase of phase ratio, the single-stage extraction efficiency of lithium first increased and then leveled off. The lithium extraction rate reached 51.04% at an organic/aqueous (O/A) phase ratio of 0.5, 87.99% at O/A = 1, and 96.57% at O/A = 2. Further increasing the phase ratio exerted no obvious influence, and the extraction rate remained stable at this level thereafter.

Table 5. Results of the three-stage cross-flow extraction experiment

Sample	Aqueous-Phase (g/L)			Organic Phase (g/L)			Extraction Efficiency (%)		
	Li	Na	K	Li	Na	K	Li	Na	K
First-Stage Extraction	0.49	64.55	10.55	2.01	0.27	-0.30	80.40	0.42	-2.93
Secondary Extraction	1.51	65.10	10.55	0.99	-0.28	-0.30	39.68	-0.43	-2.93
Three-Stage Extraction	2.44	65.00	10.30	0.06	-0.18	-0.05	2.56	-0.28	-0.49
Initial Aqueous Phase	2.50	64.82	10.25	—	—	—	—	—	—

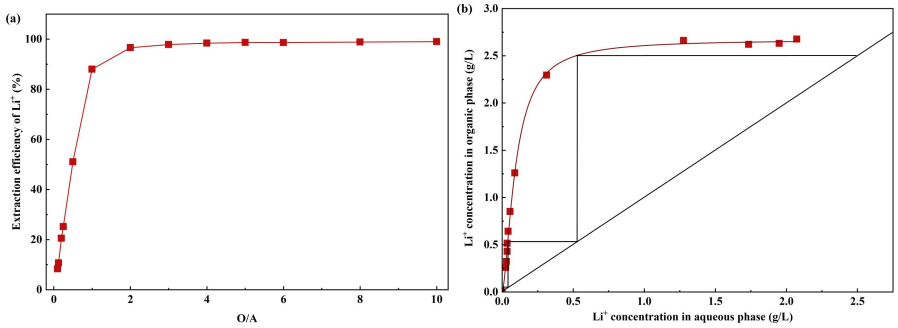

Figure. 10 Effect of phase ratio on lithium extraction efficiency and extraction equilibrium. (a) Single-stage extraction efficiency of Li^+ at different O/A phase ratios; (b) Extraction isotherm. Copyright: Created by the authors using Origin 2026 software.

Based on the investigation of different comparison conditions, the Langmuir model was used to fit the equilibrium

concentrations of Li in the aqueous and organic phases, and extraction isotherms were plotted[39,40].

$$C_{org}=\frac{K_L\times,C_{max}\times C_{aq}}{1+K_L\times C_{aq}} \quad (9)$$

Where is the maximum extraction capacity of the organic phase (g/L), is the Langmuir constant (K_L) associated with the extraction equilibrium constant, is the equilibrium concentration in the organic phase, and is the equilibrium concentration in the aqueous phase.

As shown in **Figure. 10(b)**, in the low-concentration region, the isotherms exhibit a steep slope. As the concentration increases, the slope gradually decreases, the curves become flatter, and the organic phase approaches saturation. As indicated by the fitting results, for the feed solution with a lithium concentration of 2.50 g/L, deep extraction of lithium can be accomplished by three-stage countercurrent extraction, where the residual Li^+ concentration in the raffinate is below 20 mg/L. The fitted saturated capacity of the extractant is 2.67 g/L, which shows good consistency with the experimental value acquired from three-stage cross-current extraction. The fitted constant is 64.81, demonstrating that the extractant has strong affinity for lithium and enables efficient extraction even at low concentrations.

3.4.3 Washing and Stripping Conditions

In the extraction process, washing and stripping are key steps for controlling the purity and recovery rate of products. For the present extraction system, both procedures require regulation of the hydrogen ion concentration in the aqueous phase. An excessively low H^+ concentration during washing fails to remove impurity ions effectively, while an overly high H^+ concentration will cause the loss of lithium ions. If the acid concentration for stripping is insufficient, lithium ions loaded in the organic phase cannot be fully stripped off. Conversely, an excessively high stripping acid concentration will lead to increased consumption of hydroxide ions during the recycling of the organic phase. Accordingly, dilute sulfuric acid solutions with different H^+ concentrations were adopted to conduct single-stage washing and stripping tests on the lithium-loaded extractant, so as to determine the optimal H^+ concentration. The phase ratio (O/A) was fixed at 10:1 for both washing and stripping operations. The relevant results are illustrated in the **Figure. 11**.

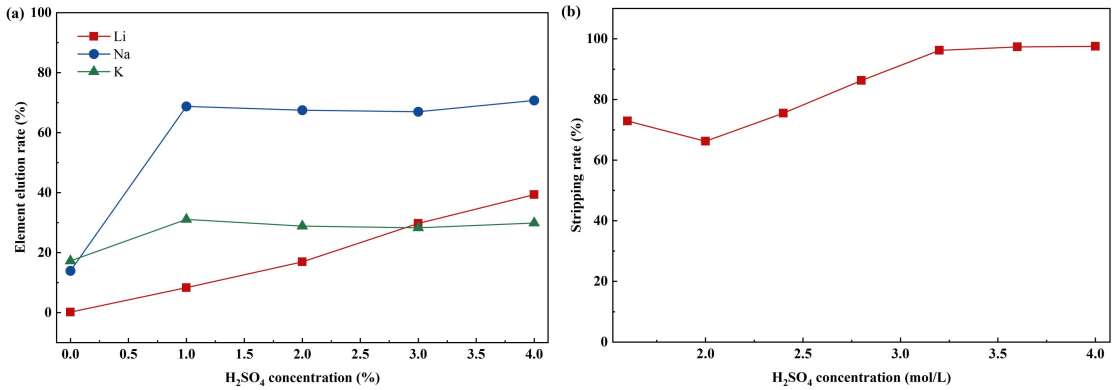

Figure. 11 Effect of acid concentration on washing and stripping performance. (a) Elution rates of Li^+, Na^+, and K^+ at different H^+ concentrations; (b) Stripping rates of Li^+ at different H^+ concentrations. Copyright: Created by the authors using Origin 2026 software.

When pure water was used for washing alone, barely any loaded lithium in the extractant was eluted, and the elution rates of sodium and potassium were both below 20%. At a sulfuric acid concentration of 1% (corresponding to an H^+ concentration of 2%), the elution rates of sodium and potassium reached 68.77% and 31.07%, respectively. These values remained nearly constant with further increase of H^+ concentration. By contrast, the elution rate of Li^+ increased linearly as the H^+ concentration rose. Therefore, the optimal H^+ concentration in the washing solution was determined to be 2%.

Based on the analysis of the extraction reaction equation above, the saturated lithium loading capacity of the extractant is equivalent to the extractant concentration, i.e., 0.40 mol/L. The theoretically required H^+ concentration for stripping is 4 mol/L (corresponding to 2 mol/L H_2SO_4), and the single-stage stripping rate under this condition is 66.22%. The stripping rate increases synchronously with the rise of acid concentration. Nevertheless, excess H^+ can be entrained into the organic phase during stripping, which will cause additional consumption of OH^- in the subsequent recycling of the extractant. Satisfactory stripping efficiency can still be achieved when using an equivalent or slightly insufficient H^+ concentration. Moreover, favorable stripping performance can be obtained by adopting the multi-stage countercurrent stripping process, which was further verified via continuous extraction experiments.

3.5 Compatibility

3.5.1 Carbonate Concentration

To further verify the extractant's ability to extract and separate lithium under different alkaline conditions, the effect of varying carbonate concentrations on the extraction efficiency was investigated. The results are shown in **Figure. 12(a)**. When the carbonate concentration exceeds 10 g/L, the lithium extraction rate can reach over 80%; at this point, the ratio of carbonate concentration to Li^+ concentration in the feed solution is approximately 0.5. As the carbonate concentration increases, the Li extraction rate stabilizes at around 90%; when the carbonate concentration exceeds 22.75 g/L, the extraction rates of Na and K begin to rise. Furthermore, as shown in **Figure. 12(b)**, the COD in the extractant raffinate increases as the carbonate concentration rises, which is a common issue with β-diketone extractants[29,30]. Compared to conventional extractants, which require highly alkaline conditions to efficiently extract lithium ions, the extractant developed in this study can achieve high-efficiency extraction under mildly alkaline conditions. This avoids increased reagent costs and reduced dissolution losses during the extraction process.

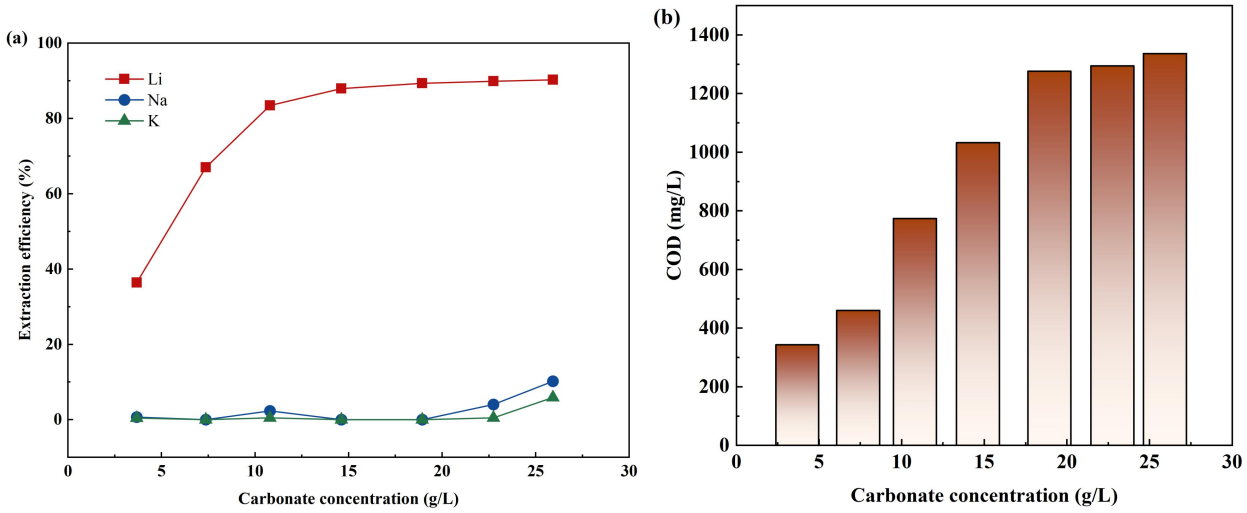

Figure. 12 Lithium extraction and separation performance at different carbonate concentrations. (a) Extraction efficiencies of Li^+, Na^+, and K^+; (b) COD values of the raffinate. Copyright: Created by the authors using Origin 2026 software.

3.5.2 Sodium Ion Concentration

The presence of inorganic salts in the feed solution may result in salting-out or solubilization effects during the extraction process, thereby impacting extraction efficiency. When dealing with different types of lithium-containing feed solutions, it is necessary to examine not only variations in alkalinity but also the effect of salt concentration on extraction performance. To simplify the analysis of the influence of salt concentration and to avoid competitive interference among multiple metal ions, the feed solution contains only Li^+ and Na^+ cations. The Na^+ concentration in the solution was increased gradually from 15 g/L to 50 g/L, while the Li^+ concentration was kept constant at 2.50 g/L. The results are shown in the **Figure. 13**. As the salt concentration increased, the single-stage extraction rates of Li^+ and Na^+ decreased only slightly: the Li^+ extraction rate decreased from 91.68% to 87.30%, and the Na^+ extraction rate decreased from 7.59% to 1.42%. After the first extraction stage, the pH of the aqueous phase remained at around 8.3. After the second stage, the equilibrium pH fluctuated within a narrow range near 7.8 (not exceeding 0.1). After the third-stage extraction, the equilibrium pH showed a slight decreasing trend as the salt concentration increased, dropping from 7.91 to 7.73. A slight salt-solubility effect occurred during the extraction process as the salt concentration increased. Although this had a slight negative impact on single-stage extraction, this negative effect can be eliminated through multi-stage extraction.

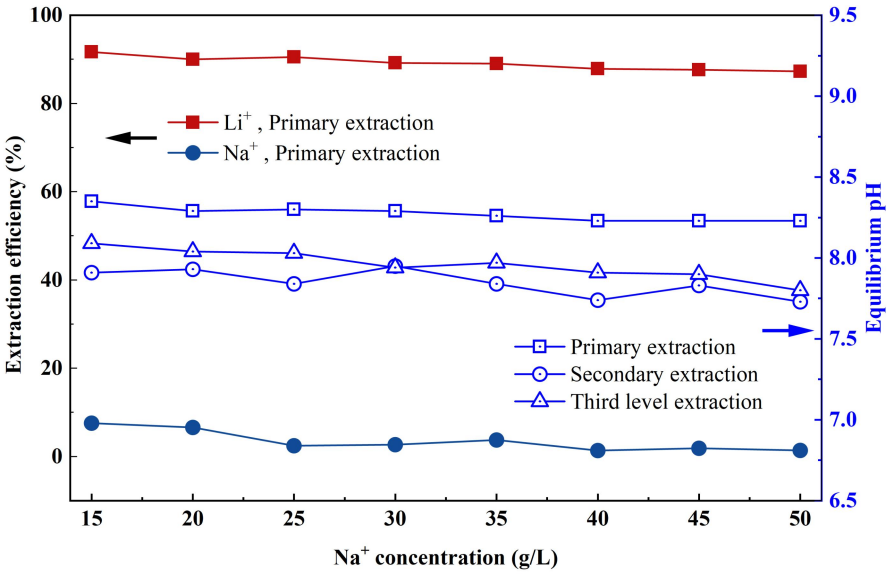

Figure. 13 Extraction Efficiency at Different Na^+ Concentrations. Copyright: Created by the authors using Origin 2026 software.

3.6 Validation of Extraction Performance

Cyclic extraction experiments were conducted on a specific feed solution system based on previous research. These experiments used three-stage countercurrent extraction, two-stage countercurrent washing and two-stage countercurrent reverse extraction; the process flow is shown in the **Figure. 14**. The extraction process has an O/A ratio of 1, while the washing and back-extraction processes have an O/A ratio of 10. No additional alkali is added during the extraction process. A 1wt% dilute sulfuric acid solution is used in the washing process, and a 2 mol/L sulfuric acid solution is used in the back-extraction process.

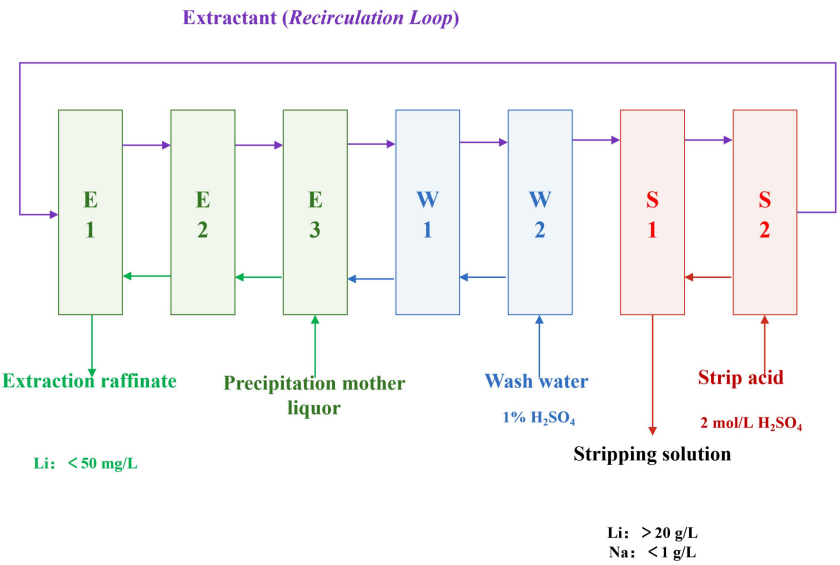

Figure. 14 Process flow for verifying the efficacy of the IPE-Z extraction agent recirculation. Copyright: Created by the authors using Microsoft PowerPoint.

The results of the cyclic experiments are presented in **Table 6**. Under alkali-free conditions, three-stage countercurrent extraction reduced the lithium concentration in the extractate to 34.10 mg/L, with an extraction efficiency of 98.70%. The extractate had a pH of 7.2 and a lithium-sodium separation factor of 478.06 and a lithium-potassium separation factor of 376.69, which indicates good separation efficiency. Furthermore, no issues such as emulsification or difficulties with phase separation were observed during the process. Following sulfuric acid back-extraction, the Li concentration in the back-extractate was 24 g/L, with a back-extraction rate of 99.80%, which indicates excellent back-extraction performance.

Table 6. Results of the circulating extraction experiment on lithium-precipitated mother liquor

State of the Extractant	Element	Extraction Raffinate mg/L	Organic Phase Load before Washing mg/L	Organic Phase Load after Washing mg/L	Stripping Solution mg/L
New Extractant	Li	45.70	2328.80	2197.90	24006
	K	9199.90	7.40	235	49.40
	Na	48087.30	211.90	17935	569.60
Recycled Extractant	Li	34.10	2309.90	2333	21470
	K	9780	45.60	14.90	22.50
	Na	51256	562	223.30	1982.20

The economic advantages of the IPE-Z/TBP system, compared with traditional alkaline extraction systems such as HBTA/TBP and Lix54, are primarily reflected in the following two aspects. Firstly, the cost of alkali consumption: traditional systems require the pH to be adjusted to ≥ 10–11, resulting in high additional alkali consumption. This system can, however, operate at the inherent alkalinity of the feed solution (extract residue pH ≈ 7.2), requiring no additional alkali to be added. This significantly reduces the cost of alkali reagents. Secondly, the cost of wastewater treatment: the extract residue from traditional high-alkali processes must be neutralised before discharge. The extract residue from this system, however, has a pH of ≈ 7.2 and can be fed directly into subsequent water treatment units. This saves on the cost of neutralising reagents and operation. The IPE-Z extractant has demonstrated stable processing performance and economic advantages in both actual and simulated feed solutions, validating its potential for industrial application in lithium-containing solutions, such as lithium precipitation mother liquors.

4. Conclusion

This study developed an extractant that can efficiently extract lithium under weakly alkaline conditions, and examined how it works. By studying the performance of the extractant in the extraction, washing, and back-extraction processes, we determined the optimal processing conditions and validated its effectiveness using actual feed solutions. The study provides comprehensive industrial application data in support of alkali-free extraction technology for the recovery of lithium from lithium-precipitated mother liquors and carbonate-type salt lakes.

(1) Based on an analysis of the energy differences between ketone and enol tautomers, as well as ESP analysis, it can be concluded that the electronic effects of substituents directly influence a molecule's enolization capacity. Considering both enolization capacity and the coordination activity of the carbonyl oxygen atom, HPMBP may offer an advantage when taking HTTA, HBTA, HDBM, and HPMBP as examples. The ability of a

molecule to undergo enolization and the distribution of localized potentials at the coordinating atoms in the enolate anion can serve as important reference criteria for the structural design of extractants.

(2) When the ratio of CO_3^{2-} to Li^+ in the feed solution reaches 0.6, highly efficient lithium extraction can be achieved. During the extraction reaction, the extractant molecules, co–extractant molecules, and lithium ions coordinate in a 1:1:1 ratio, and the extractant molecules maintain a stable structure.

(3) Using lithium-precipitated mother liquor as the extractant, with an extractant concentration of 0.40 mol/L and a saturation capacity of 3.06 g/L, the optimal number of extraction stages is three. Under an O/A ratio of 10, controlling the H^+ concentration during the washing process to 2% enables both the efficient elution of impurity ions and the minimization of lithium loss. During the back-extraction process, using an acid with a H^+ concentration of 4 mol/L enables efficient stripping of cations from the loaded organic phase.

(4) The IPE-Z/TBP co–extraction system developed in this study achieved the efficient extraction of Li^+ ions from lithium–precipitated mother liquor under low-alkali conditions. This overcomes the limitation of high alkali consumption associated with traditional lithium extractants. The optimal ratio of extractant to co-extractant is 1:4. When the extractant concentration is 0.40 mol/L, the extraction efficiency of Li^+ from the lithium precipitation mother liquor is 98.70%, with a pH of 7.2 in the extractant raffinate. This means that the extraction process requires virtually no additional alkali and the residue can be fed directly into the subsequent water treatment process. These advantages significantly reduce enterprises' environmental treatment costs and drive the green and low-carbon transition of the lithium–ion battery industry, demonstrating excellent industrial application prospects.

Author Contributions

Rongyue Wang: conceptualization, methodology, writing – original draft, writing – review & editing. Hui Li: investigation, data curation, formal analysis. Gaojie Xu: validation, methodology, writing – review & editing. Pengge Ning: resources, supervision, project administration, funding acquisition. All authors have read and approved the final manuscript and agree to be accountable for all aspects of this work.

Conflicts of Interest

The authors declare that they have no known competing financial interests or personal relationships that could have appeared to influence the work reported in this paper.

Funding

This study was supported by National Natural Science Foundation of China (Grant No. 92475115).

Data Availability

The data supporting the findings of this study are available from the corresponding author upon reasonable request.

References

[1] Wang B, Wang F, Shao C, *et al.* Bridging China's energy and mineral system: Evaluating the risk of domestic supply shortages for critical raw materials in the context of China's energy transition. *Journal of Cleaner Production*. 2026, 547: 1-14. [Google Scholar] [CrossRef]

[2] Zhang X. 2025 China's lithium battery industry production and import/export show growth. *China Nonferrous Metals News*. Available online: https://www.cnmn.com.cn/ShowNews1.aspx?id=469013 (accessed on 18 August 2026)

[3] Ge HW, Wang HY, Wang M. Solubility and Thermodynamics of Lithium Carbonate in Its Precipitation Mother Liquors. *Molecules*. 2025, 30 (17): 1-12. [Google Scholar] [CrossRef]

[4] Zhang HP, Gao Y, Tian Z, *et al.* The phosphonic acid based extraction-precipitation strategy for recovering Li from Li_2CO_3 precipitated mother liquor. *Desalination*. 2026, 623: 1-12. [Google Scholar] [CrossRef]

[5] Xiang XY, Li X, Wei YF, *et al.* Desalination of mother liquor generated from the precipitation of lithium carbonate during the recycling of retired lithium ion battery. *Desalination and Water Treatment*. 2024, 320: 1-7. [Google Scholar] [CrossRef]

[6] Li C, Liu P, Zhang X, *et al.* Separation of Li, Na, K from salinity wastewater via targeting coordination precipitation with phosphate and chlorine. *Journal of Environmental Chemical Engineering*. 2025, 13 (2): 1-10. [Google Scholar] [CrossRef]

[7] Liu YB, Ma BZ, Lv YW, *et al.* Selective synthesis of LiOH from high-sodium concentration Li_2CO_3 mother liquor. *Journal of Cleaner Production*. 2023, 430: 1-9. [Google Scholar] [CrossRef]

[8] Gao J, Deng TL, Zhu HF. A synergistic extraction system for lithium recovery from salt lake brine. No. CN102001692B, 7 November 2012.

[9] Zhu ZW, Zhang J, Wang LN, *et al.* A method for extracting lithium from lithium-containing solutions by solvent extraction. No. CN111057848A, 24 April 2020.

[10] Cao HB, Ning PG, Xu GJ, *et al.* An extractant for recovering lithium from alkaline lithium-containing solutions, and its preparation method and applications. No. CN118241039A, 25 June 2024.

[11] Dobó Z, Dinh T, Kulcsár T. A review on recycling of spent lithium-ion batteries. *Energy Reports*. 2023, 9: 6362-6395. [Google Scholar] [CrossRef]

[12] Huang K, Li J, Xu ZM. Recycling of lithium-ion batteries: recent advances and perspectives. *Journal of Power Sources*. 2018, 399: 274-286. [Google Scholar] [CrossRef]

[13] Deng Y, Chai GL, Zhang YH. Research progress on lithium extraction from salt-lake brine. *Journal of Industrial and Engineering Chemistry*. 2025, 143: 92-108. [Google Scholar] [CrossRef]

[14] He DS, Ma M. Quantum chemical study of extraction characteristics of kinetic synergist OT in liquid membrane using HPMBP as carrier. *Separation and Purification Technology*. 2013, 107: 289-296. [Google Scholar] [CrossRef]

[15] Zhang LC, Li LJ, Shi D, *et al.* Selective extraction of lithium from alkaline brine using HBTA-TOPO synergistic extraction system. *Separation and Purification Technology*. 2017, 188: 167-173. [Google Scholar] [CrossRef]

[16] Sun Q, Chen H, Yu JG. A density functional theory insight into the extraction mechanism of lithium recovery from alkaline brine by β-diketones. *American Institute of Chemical Engineers Journal*. 2023, 69 (7). [Google Scholar] [CrossRef]

[17] Zhang LC, Li LJ, Shi D, *et al.* Recovery of lithium from alkaline brine by solvent extraction with β-diketone. *Hydrometallurgy*. 2018, 175: 35-42 [Google Scholar] [CrossRef]

[18] Wang JF, Yang SC, Bai RB, *et al.* Lithium recovery from the mother

liquor obtained in the process of Li_2CO_3 production. *Industrial & Engineering Chemistry Research*. 2019, 58 (1): 1363-1370. [Google Scholar] [CrossRef]

[19] Cao JY, Meng Z, Zhang J, *et al*. Highly selective recovery of lithium from real precipitation mother liquor using HPMBP-Cyanex 923 synergistic extraction system. *ACS Sustainable Chemistry & Engineering*. 2025, 13 (45): 17902-17912. [Google Scholar] [CrossRef]

[20] Zhou GM, Yn WJ, Yan SF, et al. Lithium solvent extraction from weak alkaline brine by 2-hydroxy-5-nitro-4-alkoxy-benzophenone and TRPO. *American Institute of Chemical Engineers Journal*. 2025, 71 (4).[Google Scholar] [CrossRef]

[21] Gaussian 16, Revision A.03, Frisch, M. J, *et al*. 2016. Available online: https://gaussian.com/citation_a03/ (accessed on 18 August 2026).

[22] Zhang J, Lu T. Efficient evaluation of electrostatic potential with computerized optimized code. *Physical Chemistry Chemical Physics*. 2021, 23: 20323-20328. [Google Scholar] [CrossRef]

[23] Lu T, Chen F. Multiwfn: A multifunctional wavefunction analyzer. *Journal of Computational Chemistry*. 2012, 33: 580-592. [Google Scholar] [CrossRef]

[24] Lu T. A comprehensive electron wavefunction analysis toolbox for chemists, Multiwfn. *The Journal of Chemical Physics*. 2024, 161 (8). [Google Scholar] [CrossRef]

[25] Humphrey W, Dalke A, Schulten K. VMD: Visual Molecular Dynamics. *Journal of Molecular Graphics*. 1996, 14: 33–38. [Google Scholar] [CrossRef]

[26] Zare L, Nekoei AR, Vakili M. Insights into intramolecular hydrogen bonding and π-electron delocalization; a case study on some β-diketone compounds, with special focus on 2-furoylacetone. *Computational and Theoretical Chemistry*. 2025, 1254: 1-16. [Google Scholar] [CrossRef]

[27] Adeniyi AA, Conradie J. The stability, kinetics and inter-fragment electron communication of the tautomers of twelve selected β-diketone molecules: A computational study. *Journal of Molecular Graphics and Modelling*. 2018, 85: 25-39. [Google Scholar] [CrossRef]

[28] Adeniyi AA, Conradie J. Influence of substituents on the reduction potential and pKa values of β-diketones tautomers: A theoretical study. *Electrochimica Acta*. 2019, 297: 947-960. [Google Scholar] [CrossRef]

[29] Mathew J, Suresh CH. Use of Molecular Electrostatic Potential at the Carbene Carbon as a Simple and Efficient Electronic Parameter of N-heterocyclic Carbenes. *Inorganic Chemistry*. 2010, 49 (10): 4665-4669. [Google Scholar] [CrossRef]

[30] Bellucci L, Bottaro G, Labella L, *et al*. Composition–Thermometric Properties Correlations in Homodinuclear Eu^{3+} Luminescent Complexes. *Inorganic Chemistry*. 2020, 59 (24): 18156-18167. [Google Scholar] [CrossRef]

[31] Conradie J. Comparative Review of *O,O′*-, *N,O*-, and *N,N′*-Bidentate Ligands: Structural and Electronic Properties of β-Diketones, Enaminones, and β-Diketiminates. *Molecules*. 2026, 31 (7): 1-37. [Google Scholar] [CrossRef]

[32] Mundra SK, Pai SA, Subramanian MS. Synergistic extraction of uranyl ion with acylpyrazolones and dicyclohexano-18-crown-6. *Journal of Radioanalytical and Nuclear Chemistry*. 1987, 116: 116, 203–211. [Google Scholar] [CrossRef]

[33] Zhang XK, Zhang J, Su H, *et al*. Recovery of lithium from the mother solution of lithium precipitation in lithium ore processing. *Rare Metals*. 2022, 46 (01): 67-77. (in Chinese) [DOI]

[34] Zhao JX, Chen H, Yu JG. Selective lithium recovery from lithium precipitation mother liquor by using a diketone-based solvent. *Desalination*. 2024, 591: 1-10. [Google Scholar] [CrossRef]

[35] Ji LM, Shi D, Peng XW, *et al*. Lithium extraction from carbonate-rich Salt Lake brine using HBTA/TBP system. *Rare Metals*. 2024, 43: 6717-6729. [Google Scholar] [CrossRef]

[36] Chen W, Li XW, Chen LL, *et al*. Tailoring hydrophobic deep eutectic solvent for selective lithium recovery from the mother liquor of Li_2CO_3. *Chemical Engineering Journal*. 2021, 420 (2): 1-9. [Google Scholar] [CrossRef]

[37] Zhang L, Li J, Ji L, *et al*. Separation of lithium from alkaline solutions with hydrophobic deep eutectic solvents based on β-diketone. *Journal of Molecular Liquids*. 2021, 344: 1-9. [Google Scholar] [CrossRef]

[38] Zhang J, Liu Y, Liu W, *et al*. Mechanism study on the synergistic effect and emulsification formation of phosphine oxide with β-diketone for lithium extraction from alkaline systems. *Separation and Purification Technology*. 2021, 279: 1-10. [Google Scholar] [CrossRef]

[39] Poposka FA, Nikolovski K, Tomovska R. Equilibria and mathematical models of extraction of citric acid with isodecanol/n-paraffins solutions of trioctylamine. *Journal of Chemical Engineering of Japan*. 1997, 30 (5): 777-785. [Google Scholar] [CrossRef]

[40] Testard F, Berthon L, Zemb T. Liquid–liquid extraction: An adsorption isotherm at divided interface?. *Comptes Rendus Chimie*. 2007, 10 (10-11): 1034-1041. [Google Scholar] [CrossRef]